Mafld Causes Alterations in Thalamus Energy Metabolism and Brain Structure

Saverio Nucera
University Magna Graecia
Stefano Ruga
University Magna Graecia
Antonio Cardamone
University Magna Graecia
Anna Rita Coppoletta
University Magna Graecia
Lorenza Guarnieri
University Magna Graecia
Maria Caterina Zito
University Magna Graecia
Francesca Bosco
University Magna Graecia
Roberta Macrì
University Magna Graecia
Federica Scarano
University Magna Graecia
Miriam Scicchitano
University Magna Graecia
Jessica Maiuolo
University Magna Graecia
Cristina Carresi
University Magna Graecia
Rocco Mollace
University Magna Graecia
Luca Cariati
University Magna Graecia
Giuseppe Mazzarella
Magna Graecia University
Ernesto Palma
University Magna Graecia
Micaela Gliozzi (gliozzi@unicz.it)

University Magna Graecia
Vincenzo Musolino
University Magna Graecia
Giuseppe Lucio Cascini
Magna Graecia University
Vincenzo Mollace
University Magna Graecia

Research Article

Keywords: MAFLD, NASH, MAFLD, NC NW, DIAMOND, NAFLD, hepatocellular carcinoma (HCC), thalamus, hippocampus, pre-frontal cortex

Posted Date: July 19th, 2021

DOI: https://doi.org/10.21203/rs.3.rs-712539/v1

Abstract

Background

Metabolic associated fatty liver disease (MAFLD), commonly known as non-alcoholic fatty liver disease, represents a continuum of events characterized by excessive hepatic fat accumulation which can progress to nonalcoholic steatohepatitis (NASH), fibrosis, cirrhosis, and in some severe cases hepatocellular carcinoma. MAFLD might be considered as a multisystem disease that affects not only the liver but involves wider implications, relating to several organs and systems, the brain included. The present study aims to investigate changes associated with MAFLD-induced alteration of thalamic metabolism *in vivo*.

Methods

DIAMOND mice were fed a chow diet and tap water (NC NW) or fat Western Diet (WD SW) for up to 28 weeks. At the baseline and weeks 4, 8, 20, 28 the thalamic neurochemical profile and total cerebral brain volume were evaluated longitudinally in both diet groups using ^{1}H-MRS. To confirm the disease progression, at each time point, a subgroup of animals was sacrificed, the livers excised and placed in formalin. Liver histology was assessed and reviewed by an expert liver pathologist.

Results

MAFLD development significantly increases the thalamic levels of total N-acetylaspartate, total creatine, total choline, and taurine. Furthermore, in the WD SW group a reduction in total cerebral brain volume has been observed ($p < 0.05$ vs NC NW).

Conclusion

Our results suggest that thalamic energy metabolism is affected by MAFLD progression. This metabolic imbalance, that is quantifiable by ^{1}H-MRS *in vivo*, might cause structural damage to brain cells and dysfunctions of neurotransmitter release.

Introduction

Metabolic (dysfunction)-associated fatty liver disease (MAFLD)[1,2] formerly known as non-alcoholic fatty liver disease (NAFLD)[3] is a heterogeneous condition of fatty liver disease which might be influenced by multiple factors including age, gender, hormonal status, ethnicity, diet, alcohol intake, smoking, genetic predisposition, the microbiota and metabolic status[4]. The spectrum of the disease extends from steatosis to hepatocellular carcinoma (HCC)[5] and though hepatic steatosis is highly prevalent, inflammation

occurs only in a minority. Moreover, liver-related complications (i.e., cirrhosis or cancer) are likely in patients with steatohepatitis[6], but the progression is not inevitable or consequential. Indeed, cirrhosis is not a fundamental stage for HCC development[7].

This heterogeneity also underlines the possible impact of MAFLD on several organs and systems, included the brain. In fact, nervous dysfunctions[8], brain lesions, changes in perfusion and brain activity[9], brain aging, increased risk of ischemic and hemorrhagic stroke[10,11] are some of the consequences of the wide spectrum of extrahepatic alterations induced by MAFLD.

In particular, oxidative stress, in the disease progression, leads to alterations in mitochondrial function and structure with a consequent reduction in neuronal metabolism[12,13,14]. In turn, the alteration of metabolic activity in specific brain areas (i.e., thalamus, hippocampus, pre-frontal cortex) could cause cognitive deficits[15] because various metabolites, such as N-acetylaspartate, creatine, choline, glutamate and taurine[16,17,18,19] are involved in energy metabolism and in the maintenance of brain functions[20].

Changes in the cerebral levels of those metabolites, following a fatty diet, have been reported in preclinical studies[21] and evidence exists that the consumption of a high caloric diet also leads to high concentrations of inflammatory cytokines in the brain, resulting in microgliosis, astrocytosis and neuronal damage[22,8]. Moreover, patients suffering from steatohepatitis have a reduced brain volume[23] and are at higher risk to suffer from neurological diseases, which are, most probably, related to the volume reductions as well[24].

Altogether, these discoveries provide a rationale to further evaluate the role of MAFLD in brain damage, through the identification, visualization and quantification of brain biochemical markers and neurotransmitters, and the alteration of the brain volume that, overall, could reflect physiologic or pathologic conditions[25]. In this perspective, advances in neuroimaging provide unique opportunities to evaluate brain structure, biochemistry and function[26]. In particular, the proton magnetic resonance spectroscopy (^{1}H-MRS) represents a non-invasive method useful to study brain metabolism, longitudinally and in a non-invasive manner[27].

Therefore, the aim of our work was to analyze the total brain volume in a diet-induced animal model of non-alcoholic fatty liver disease (DIAMOND)[28] and to assess and quantify the main metabolites present in brain tissue, including N-acetylaspartate (NAA), the predominant MRS signal in the healthy neurons[16]; total creatine (tCr), involved in cellular energy metabolism; total choline (tCho), also involved in the synthesis and the breakdown of cellular membranes[29]; the neuroinflammation modulator taurine (Tau)[30,31] and the excitatory neurotransmitter glutamate (Glu)[32]. As the concentration of brain metabolites often reflects the state of its metabolic activity and energetic status, the ^{1}H-MRS analysis of the metabolic fluctuation might be predictive of the potential MAFLD implications at brain level.

Materials And Methods

Animals. Male DIAMOND (diet-induced animal model of non-alcoholic fatty liver disease) mice were purchased from Sanyal Biotechnology (Virginia Beach, VA, USA) kept under standard laboratory conditions in a specific-pathogen-free animal facility and maintained at 22 ± 2°C with alternating 12 h light–dark cycle. All the experimental procedures were performed according to protocols approved by the Animal Care of University Magna Graecia of Catanzaro. The experimental procedures were carried out in compliance with the ARRIVE guidelines. All experiments were performed in accordance with the European Commission guidelines (Directive 2010/63/EU) for the animals used for scientific purposes.

Study design. Mice of 8–12 weeks of age and weight of 20.54 ± 0.53 grams were divided into two groups and fed *ad libitum* a normal chow diet (NC, Harlan TD.2019) and tap water (NW) or a high fat/high carbohydrate diet (Western diet, WD, Harlan TD.88137) with a high fructose-glucose water solution (SW, 23.1 g/L d-fructose + 18.9 g/L d-glucose) for up to 28 weeks. The choice of the animals and the diet used to develop steatosis and steatohepatitis have been based on previously published studies[6,28]. One day before starting diet regimen, baseline body weight and MRS were assessed. On weeks 4, 8, 20 and 28, thalamic neurochemical profile was evaluated in the two diet cohorts using ^{1}H-MRS. Animals body weight was assessed weekly. The day of the sacrifice, animals were exposed to inhaled isoflurane prior to being euthanized. Euthanasia was performed by cervical dislocation. The entire liver was removed from the abdominal cavity and weighed. The liver was sectioned in a sagittal plane and placed in containers of 10% formalin, for later histologic processing and analysis.

^{1} H-MRS. Before MRS acquisition, mice were anesthetized with 4% of isoflurane (Forane, Abbott) vaporized in O_2 (flow: 2 l/min). During acquisition, anesthesia was kept between 1,5–2% to maintain the breathing rhythm (SA Instruments, Inc., Stony Brook, NY, USA) between 50 and 80 breaths per minute. Body temperature was monitored and maintained at 37°C (SA Instruments, Inc., Stony Brook, NY, USA).

^{1}H-MRS spectra were acquired with a Bruker Pharmascan 70/16 US 7T bore MR scanner (Bruker Biospin MRI GmbH, Ettlingen, Germany), equipped with a Bruker's MRI CryoProbe™ with MRI cryocooler, in order to increase signal-noise-ratio and reach a higher sensitivity than standard room temperature RF coils.

Initially, a localizer acquisition was performed for the purpose of center mouse brain in the imaging field of view. Subsequently, Axial and Sagittal T2_turboRARE weighted images with fat suppression (TE: 35 ms, TR: 2500 ms, averages: 2, thickness of 0.7 mm, slices 9, field of view 20x20 mm^2, data matrix 256x256) were used to place the voxel accurately in the thalamic region. The thalamic voxel (2x2x2 mm^3) was positioned based upon referencing a mouse brain atlas. A localized shimming procedure was performed to improve the B_0 field map homogeneity in the region of interest. Then, a variable power and an optimized relaxation delays (VAPOR) were applied as water suppression scheme.

^{1}H-MRS data were acquired with a PRESS_1H sequence with the following parameters: TE 16.6 ms, TE1 8.99 ms, TE2 7.61, TRd 2500 ms, averages 256, dummy scans 2, VOI 2x2x2 mm^3.

^{1}H-MRS data analysis was performed using TARQUIN 4.3.10, a new accurate and robust modeling algorithm[33] which allows to quantify the concentrations of metabolites within the voxel.

Volumetric Analysis. Volumetric analysis was performed using OsiriX imaging software (v. 12.0.2, Pixmeo SARL, Switzerland). Total cerebral brain volumes (TCBVs) were estimated using T1_FLASH_3D images in coronal view with a thickness of 112.78 µm per slice, obtained with a T1_FLASH_3D_iso sequence (TE: 8 ms, TR: 50 ms, averages: 1, dummy scans: 20, image size: 133x133x80, field of view: 15x15x10 mm^3). By the "Draw tool" the ROIs were traced on the MRI sections. To improve the viewing of cerebral margins, a Default WL / WW, "French Clut" and a linear opacity table were used. Total brain's area was defined every 3 slices, starting from the olfactory bulbs up to the last part of the cerebellum. Subsequently, "Generate Missing ROIs" function was used to outline total brain area for all slices. Then, "Compute ROI Volume" feature was used to merge the ROIs of the entire brain and estimate its volume.

Histological analysis. Liver histology was assessed from paraffin-embedded tissue sections stained with hematoxylin and eosin. Histology was reviewed using the NASH-Clinical Research Network (CRN) criteria and fatty liver inhibition of progression (FLIP) algorithm by a liver pathologist.

For each liver slide, the main histological lesions were assessed using the Steatosis-Activity-Fibrosis (SAF) score system[34,35,6]. Steatosis was graded on a scale of 0 to 3 (0: < 5%; 1: 5–33%; 2: 34–66%; 3: >67%). Grade of activity (0–2) is given by the sum between the presence of ballooning and inflammation. Ballooning hepatocytes was graded as 0 (none), 1 (when few hepatocytes presented a rounded shaped, reticulated, and pale cytoplasm, but with normal dimensions), and 2 (when there is a cluster of prominent ballooning hepatocytes).

The presence of inflammatory foci within the lobule or within the sinusoids, was graded as 0 (none), 1 (< 2 foci per 20x field), 2 (2–4 foci per 20x field), and 3 (> 4 foci per 20x field). The NAFLD activity score (NAS) was calculated by addition of grades of steatosis, inflammation, and ballooning[5]. Steatohepatitis has been diagnosed as previously described[28].

Statistical analysis. Data were analyzed with GraphPad PRISM 9.1.2 (GraphPad Software, Inc., La Jolla, CA, USA). All results were expressed as mean ± S.E.M. (Standard error of the mean). Normality was tested using Shapiro-Wilk normality test. Normally distributed data were analyzed by one way ANOVA followed by Tukey's test, while data without normal distribution were analyzed using Kruskal–Wallis analysis of variance and subsequent Dunn's tests. The Unpaired Two-tailed Student's *t* test was used for comparison of data derived from two groups. Value with $p < 0.05$ were considered statistically significant. Correlation analysis was assessed using Spearman's correlation coefficient, using NAS as pathology marker.

Results

Mice fed a high fat diet and sugar water develop NAFLD. Animals fed a WD SW developed obesity compared to CD NW-fed mice (Fig. 1A). The weight gain was accompanied by an increase in liver weight

at all time points (Fig. 1B).

Mice on a high fat diet with *ad libitum* sugar water administration developed steatohepatitis (Fig. 1C,D), which was characterized by steatosis, lobular inflammation, and hepatocellular ballooning (Fig. 1D,E). The NAFLD activity score (NAS) increased by week 8 and remained higher than NC NW mice by week 28 (Fig. 1E). Specifically, histology of the liver showed an extensive development of steatosis by week 8 in WD SW-fed mice (Fig. 1D,E). At 8 weeks mice had a mean steatosis grade of 2.5 ± 0.3 (Fig. 1E) with 60 ± 11% cells with steatosis (not shown). This remained nearly constant after 20 weeks, with a mean steatosis grade of 2.7 ± 0.1 (Fig. 1E), and 68.75 ± 4.7% cells with steatosis (not shown). At week 28 weeks mice had a mean steatosis grade of 2.9 ± 0.1 (Fig. 1E) and 81 ± 3.4% cells with steatosis (not shown). Following initiation of WD SW diet, steatohepatitis developed in almost all mice and at week 20, all mice had NASH with a prominent inflammation (Fig. 1C,D,E), whereas at week 28, 8 out of 10 mice developed steatohepatitis (Fig. 1C). Stage 1 fibrosis was present by week 20 after initiation of the WD SW diet (Fig. 1E). In contrast, none of the animals on chow diet developed NAFLD (Fig. 1C).

Volumetric Analysis of control and high-fat diet-fed animals. Volumetric analysis showed the same total cerebral brain volumes (TCBVs) in both animal cohorts at 0 weeks.

The results of volumetric analysis (Fig. 2) showed a statistically significant increase in TCBVs in NC NW group after 28 weeks (0.4653 ± 0.002626 cm^3, $p < 0.01$) (Fig. 3).

In WD SW-fed animals, a statistically significant decrease of TCBVs after 28 weeks of high-fat diet has been observed (0.4307 ± 0.004573 cm^3, $p < 0.05$, Fig. 3). Moreover, comparisons of TCBVs at specific times showed a decrease at 4 weeks ($p < 0.01$), 8 weeks ($p < 0.001$), 20 weeks ($p < 0.001$) and 28 weeks ($p < 0.01$) respectively WD SW cohort compared to the control group (Fig. 3).

Smaller total cerebral brain volumes were associated with Steatosis and Steatohepatitis. Smaller TCBVs were strongly correlated with high NAS ($r = -0.9120$; $p < 0.001$, Fig. 4A) already after 8 weeks (steatosis). A strong correlation between TCBV and NAFLD was also observed during the progression of the disease either after 20 weeks ($r = -0.9415$; $p < 0.001$, Fig. 4B) either after 28 weeks ($r = -0.9498$; $p < 0.001$, Fig. 4C)

^{1}H-MRS of control and high-fat diet-fed animals. ^{1}H-MRS spectra of the mouse thalamus (Fig. 5A) for the NC NW and WD SW animals underlined the presence of the main brain metabolites between 0.7–4 PPM (Fig. 5B). The quantification of ^{1}H-MRS spectra (Fig. 5B) showed similar concentrations at the baseline in both cohorts (Fig. 6).

In the NC NW group, no significant changes occurred in metabolites concentration during the 28 weeks of the experiment, except for tNAA (6.446 ± 0.2734 mM, $p < 0.05$), tCr (7.641 ± 0.1370 mM, $p < 0.05$), Glu (8.236 ± 0.2362 mM, $p < 0.05$) and Glx (13.250 ± 0.5972 mM, $p < 0.05$), which were significantly higher at 4 weeks. Furthermore, the concentrations of tCr (7.569 ± 0.1625 mM, $p < 0.05$) and tCho (2.247 ± 0.06296 mM, $p < 0.05$) augmented at 8 weeks as well as the concentration of Tau (6.412 ± 0.3523 mM, $p < 0.05$) at 20 weeks of diet (Fig. 6).

In the WD SW group, the concentrations of tNAA (6.23 ± 0.2586 mM, $p < 0.01$), tCr (7.6 ± 0.156 mM, $p < 0.001$), Glu (7.659 ± 0.2452 mM, $p < 0.05$) and Tau (6.422 ± 0.2252 mM, $p < 0.05$) were significantly increased after 8 weeks of diet (Fig. 6). The concentrations of tNAA (6.469 ± 0.2612 mM, $p < 0.001$), tCr (8.088 ± 0.172 mM, $p < 0.001$), tCho (2.238 ± 0.04864 mM, $p < 0.05$), Glu (7.711 ± 0.2265 mM, $p < 0.05$), Glx (11.64 ± 0.3739 mM, $p < 0.05$) and Tau (6.897 ± 0.2493 mM, $p < 0.05$) were significantly increased after 20 weeks of high-fat diet (Fig. 6).

Likewise, the concentrations of tNAA (7.269 ± 0.2974 mM, $p < 0.001$), tCr (8.452 ± 0.1503 mM, $p < 0.001$), tCho (2.437 ± 0.04331 mM, $p < 0.001$), Glu (8.693 ± 0.285 mM, $p < 0.001$), Glx (12.760 ± 0.4151 mM, $p < 0.001$) and Tau (6.930 ± 0.3267 mM, $p < 0.05$) were significantly increased after 28 weeks of high-fat diet (Fig. 6).

Comparisons at specific times showed that the concentrations of tNAA ($p < 0.05$) and tCr ($p < 0.01$) were significantly higher in the WD SW group than in the NC NW control group at 20 weeks, as well as the concentrations of tNAA ($p < 0.05$), tCr ($p < 0.01$), tCho ($p < 0.05$) and Glu ($p < 0.05$) were significantly increased in the WD SW than NC NW cohort at 28 weeks (Fig. 6).

Discussion

NAFLD includes a wide spectrum of liver diseases, starting with the accumulation of lipid molecules in hepatocytes and evolving into NASH state that can degenerate to liver cirrhosis and/or hepatocellular carcinoma[5,6]. Despite the main feature is liver dysfunction, the detrimental impact of lipid accumulation can affect the whole metabolic state also predisposing to cardiovascular and neurological diseases[36]. In this view, the aim of our study was to investigate the effects of the altered lipid metabolism induced by NASH in the thalamus. In particular, we monitored and quantified over time the putative indicator of inflammation Taurine, and the levels of Glutamate, tNAA, tCho, tCr to study the impact of metabolic fluctuation on brain energetic status, structure and function.

In the global population, NAFLD prevalence is estimated around 25% although its systemic impact on body metabolism can expand this valuation to a wide population[37]. Thus, recently, it has been coined a new definition of this pathological state known as MAFLD[2]. In this context, a high-fat diet is considered the main cause of a range of systemic dysfunctions that include a gain of weight and fasting glucose, abnormal fasting insulin levels, raised lipid biosynthesis in the liver, elevated levels of circulating fatty acids and glucose intolerance[38].

The occurrence of these events was studied in depth in an animal model of MAFLD resembling the human features of disease development[39], confirming that chronic intake of a diet enriched in fats and carbohydrates contributes to induce inflammation and oxidative damage primarily to the hepatic microcirculation and then, at systemic level[40,41]. This suggests a more generalized endothelial dysfunction, also involving blood-brain barrier that, once damaged, permits the infiltration of circulating inflammatory cells into the brain[42].

In accordance with this latter hypothesis, recent studies have shown that ceramides and other toxic lipids, generated by the liver during NASH, are able to mediate adverse effects in the brain, due to their ability to cross the blood brain barrier and, consequently, to cause neuroinflammation, oxidative stress, metabolic impairment and neurotransmitter transmission deficit[43,44].

The occurrence of steatosis, lobular inflammation and hepatocellular ballooning, characterizing WD SW-induced NASH in our experiments, further support the hypothesis of its possible impact on the brain, as shown by the strong correlation between the reduction of brain volume and MAFLD progression, overtime.

At thalamic level, the detrimental role of inflammation and oxidative stress, subsequent to high fat diet consumption, has been highlighted by the onset of microgliosis and astrocytosis, contributing to neuronal damage[8] and that can progress in apoptotic death after the alteration of oxidative phosphorylation and mitochondrial dysfunction[14].In addition, similarly to other brain area, such as prefrontal cortex, hippocampus, amygdala and mammillary bodies, the alteration of metabolic activity in the thalamus also cause a functional impairment, particularly cognitive deficits characterized by memory and learning disorders[15].

Spectroscopic analysis, carried out in thalamus of high-fed diet mice, showed a time-dependent increase in the concentration of taurine, considered a hypothetical marker of inflammation, up to twentieth week. This gradual increase was accompanied, until the end of the experiment, by an enhancement in total choline which, normally, represents the sum of the levels of glycerophosphorylcholine and phosphorylcholine, both precursors of phosphatidylcholine and sphingomyelin[45,46,31].

Taken together, these results indicate that the solubilization of glycerophosphorylcholine and phosphorylcholine, probably due to oxidative/inflammatory insults affecting membranes, could be responsible not only for neuronal demyelination, but also for the alteration of plasma membrane permeability and polarization, and for the dysfunction of neurotransmitter vesicular release[47,48,49,29]. Furthermore, the same structural membrane alteration of astrocytes and microglia could affect their function, too[50].

At the end of the experiment, in thalamus of WD SW mice, increased NAA and glutamate levels were also highlighted, although they were not associated with any changes in glutamine levels (data not shown). This suggests that, in the presence of increased glucose tolerance and increased levels of circulating fatty acids, as typically observed at that time point in DIAMOND mice[28], cerebral tissue activates an alternative mechanism to the use of glucose, capable to equally satisfy its energy needs. Indeed, although glucose has always been recognized as the primary source of brain energy, growing evidence shows that other metabolites, such as glutamate and acetate, are used as energy sources, mainly by astrocytes, both in physiological and pathological conditions[51]. In this perspective, the increase in astrocytic glutamate could represent the substrate needed to an anaplerotic reaction aimed to ensure the right homeostasis of Krebs cycle and to the production of necessary lactate for neuronal survival.

The use of glutamate as a mitochondrial substrate[52,53,54] in turn, could justify its vesicular depletion at synaptic level. Consequently, the lack of glutamate release, compared to the unchanged levels of glutamine measured over time, could explain the cognitive deficits characterizing NASH[55].

In conditions of impaired metabolism, the brain can also use free fatty acids to produce energy[56]. Thus, it is plausible that astrocytes further compensate the energy deficit due to decreased glucose levels through fatty acid β-oxidation.

The main source of free fatty acids crossing the blood brain barrier may come from long-chain fatty acid/albumin complexes and, to a lesser extent, from circulating lipoproteins[56]. Once inside the astrocytes, the conversion into acetyl-CoA, operated by the acyl-CoA synthetase, allows its translocation into the mitochondrial matrix for β-oxidation and for the production of ketone bodies, such as acetoacetate, beta-hydroxybutyrate and acetone that results from their spontaneous decomposition[57]. Ketone bodies are synthesized starting from two acetyl-CoA molecules also at the peripheral level, mainly by the liver, especially in conditions of decreased glucose bioavailability. Subsequently, they are transported to the extrahepatic tissues, where they are used, after conversion into acetyl-CoA and introduction into the cycle of tricarboxylic acids, for energy production[58].

Therefore, the ketone bodies produced by astrocytes or coming from the bloodstream in conditions of more marked metabolic alterations migrate within neurons, where they are converted into acetyl-CoA and used in the Krebs cycle. On the other hand, acetyl-CoA excess is converted into NAA and stored inside neuronal mitochondria for satisfying a possible sudden increase in energy needs[59].

In our experiments, the increased amount of NAA, found in thalamus of mice fed a high-fat diet, were also associated with a raise of creatine/phosphocreatine levels, indicating also the formation of phosphate reservoirs needed for ATP synthesis.

Overall, the production of NAA and creatine/phosphocreatine appears necessary to constantly ensure correct mitochondrial functionality and, consequently, the energy needed for brain functions potentially compromised by the inflammatory insult triggered at the peripheral level by NASH. On the other hand, the tight correlation between reduced brain volume and NAFLD development, revealed by our experiments, further supports the hypothesis of an increased risk of functional deficits of specific brain areas.

Therefore, since the thalamus represents a key element in the integration of neuronal impulses within the network including prefrontal cortex, hippocampus, amygdala and mammillary bodies, a constant energy supply must be always maintained[60].

In this scenario, the use of newly synthesized glutamate as an energy source, rather than as a neurotransmitter reserve, could represent a key element for the compensation of the energetic deficit to prevent neuronal damage, but at the same time, the triggering cause of the learning and memory deficits that are often found in NASH affected patients[15].

Finally, our results also suggest the need for pharmacological interventions aimed to counteract inflammatory degeneration of MAFLD which, despite being a very widespread phenomenon with detrimental consequences at CNS level, is still not treated with a specific therapy.

Declarations

Acknowledgements

This work has been supported by PON-MIUR 03PE000_78_1 and PONMIUR 03PE000_78_2. POR Calabria FESR FSE 2014–2020 Asse 12-Azioni 10.5.6 e 10.5.12

Author contributions

V.M., G.L.C, M.G. and Vincenzo Musolino conceptualized and designed the study. S.N., S.R., A.C., A.R.C. and L.C. performed magnetic resonance spectroscopy. F.S. performed liver staining. S.N., S.R., A.C., A.R.C., L.G., M.C.Z., F.B., R.M., F.S., M.S., J.M., C.C., R.M., L.C. and G.M. performed experiments. S.R., M.C.Z. and A.C. analyzed the data. Vincenzo Musolino, R.M., E.P., M.G., G.L.C. and V.M. interpreted the data. Vincenzo Musolino, M.G. and A.C. wrote the manuscript. G.L.C. and V.M. reviewed the manuscript.

Competing interests

The authors declare no conflict of interest.

References

1. Eslam, M., Sanyal, A. J. & George, J. International Consensus Panel. MAFLD: A Consensus-Driven Proposed Nomenclature for Metabolic Associated Fatty Liver Disease. Gastroenterology 158, 1999–2014.e1(2020).
2. Fouad, Y. *et al.* The NAFLD-MAFLD debate: Eminence vs evidence. *Liver Int*, **41**, 255–260 (2021).
3. Chen, Y. *et al.* Prevalence of and risk factors for metabolic associated fatty liver disease in an urban population in China: a cross-sectional comparative study. *BMC Gastroenterol*, **21**, 212 (2021).
4. Estes, C., Razavi, H., Loomba, R., Younossi, Z. & Sanyal, A. J. Modeling the epidemic of nonalcoholic fatty liver disease demonstrates an exponential increase in burden of disease., **67**, 123–133 (2018).
5. Kleiner, D. E. *et al.* Design and validation of a histological scoring system for nonalcoholic fatty liver disease., **41**, 1313–1321 (2005).
6. Musolino, V. *et al.* Bergamot Polyphenols Improve Dyslipidemia and Pathophysiological Features in a Mouse Model of Non-Alcoholic Fatty Liver Disease. *Sci Rep*, **10**, 2565 (2020).
7. Guzman, G. *et al.* Does nonalcoholic fatty liver disease predispose patients to hepatocellular carcinoma in the absence of cirrhosis. *Arch Pathol Lab Med*, **132**, 1761–1766 (2008).
8. Bélanger, M., Allaman, I. & Magistretti, P. J. Brain energy metabolism: focus on astrocyte-neuron metabolic cooperation. *Cell Metab*, **14**, 724–738 (2011).

9. Lombardi, R., Fargion, S. & Fracanzani, A. L. Brain involvement in non-alcoholic fatty liver disease (NAFLD): A systematic review. *Dig Liver Dis*, **51**, 1214–1222 (2019).
10. Abdeldyem, S. M., Goda, T., Khodeir, S. A., Abou Saif, S. & Abd-Elsalam, S. Nonalcoholic fatty liver disease in patients with acute ischemic stroke is associated with more severe stroke and worse outcome. *J Clin Lipidol*, **11**, 915–919 (2017).
11. Mahfood Haddad, T., Hamdeh, S., Kanmanthareddy, A. & Alla, V. M. Nonalcoholic fatty liver disease and the risk of clinical cardiovascular events: A systematic review and meta-analysis. *Diabetes Metab Syndr*, **11** (Suppl 1), S209–S216 (2017).
12. García-Ruiz, C. & Fernández-Checa, J. C. Mitochondrial Oxidative Stress and Antioxidants Balance in Fatty Liver Disease. *Hepatol Commun*, **2**, 1425–1439 (2018).
13. Paradies, G., Paradies, V., Ruggiero, F. M. & Petrosillo, G. Oxidative stress, cardiolipin and mitochondrial dysfunction in nonalcoholic fatty liver disease. *World J Gastroenterol*, **20**, 14205–14218 (2014).
14. Desjardins, P. & Butterworth, R. F. Role of mitochondrial dysfunction and oxidative stress in the pathogenesis of selective neuronal loss in Wernicke's encephalopathy. *Mol Neurobiol*, **31**, 17–25 (2005).
15. Higarza, S. G. *et al.* Neurobehavioral dysfunction in non-alcoholic steatohepatitis is associated with hyperammonemia, gut dysbiosis, and metabolic and functional brain regional deficits. *PLoS One*, **14**, e0223019 (2019).
16. Daniele, G. *et al.* Plasma N-Acetylaspartate Is Related to Age, Obesity, and Glucose Metabolism: Effects of Antidiabetic Treatment and Bariatric Surgery. *Front Endocrinol (Lausanne)*, **11**, 216 (2020).
17. Beal, M. F. Neuroprotective effects of creatine., **40**, 1305–1313 (2011).
18. Zheng, Y. *et al.* Metabonomic profiles delineate potential role of glutamate-glutamine cycle in db/dbmice with diabetes-associated cognitive decline. *Mol Brain*, **9**, 40 (2016).
19. Shivaraj, M. C. *et al.* Taurine induces proliferation of neural stem cells and synapse development in the developing mouse brain. *PLoS One*, **7**, e42935 (2012).
20. Sonnay, S., Gruetter, R. & Duarte, J. M. N. How Energy Metabolism Supports Cerebral Function: Insights from 13C Magnetic Resonance Studies In vivo. *Front Neurosci*, **11**, 288 (2017).
21. Lizarbe, B., Soares, A. F., Larsson, S. & Duarte, J. M. N. Neurochemical Modifications in the Hippocampus, Cortex and Hypothalamus of Mice Exposed to Long-Term High-Fat Diet. *Front Neurosci*, **12**, 985 (2018).
22. Horvath, T. L. *et al.* Synaptic input organization of the melanocortin system predicts diet-induced hypothalamic reactive gliosis and obesity. *Proc Natl Acad Sci U S A*, **107**, 14875–14880 (2010).
23. Weinstein, G. *et al.* Association of Nonalcoholic Fatty Liver Disease With Lower Brain Volume in Healthy Middle-aged Adults in the Framingham Study. *JAMA Neurol*, **75**, 97–104 (2018).
24. Williamson, J. B. *et al.* Cerebral Metabolite Concentrations Are Associated With Cortical and Subcortical Volumes and Cognition in Older Adults. *Front Aging Neurosci*, **12**, 587104 (2020).

25. Zahr, N. *et al.* In Vivo Evidence for Alcohol-Induced Neurochemical Changes in Rat Brain Without Protracted Withdrawal, Pronounced Thiamine Deficiency, or Severe Liver Damage. Neuropsychopharmacol 34, 1427–1442(2009).
26. Hoon, A. H., Belsito, K. M. & Nagae-Poetscher, L. M. Neuroimaging in spasticity and movement disorders. *J Child Neurol*, **18** (Suppl 1), S25–39 (2003).
27. Xu, S. *et al.* In vivo high-resolution localized (1) H MR spectroscopy in the awake rat brain at 7 T. *Magn Reson Med*, **69**, 937–943 (2013).
28. Asgharpour, A. *et al.* A diet-induced animal model of non-alcoholic fatty liver disease and hepatocellular cancer. *J Hepatol*, **65**, 579–588 (2016).
29. Aureli, M., Grassi, S., Prioni, S., Sonnino, S. & Prinetti, A. Lipid membrane domains in the brain. *Biochim Biophys Acta*, **1851**, 1006–1016 (2015).
30. Jakaria, M. *et al.* Taurine and its analogs in neurological disorders: Focus on therapeutic potential and molecular mechanisms. *Redox Biol*, **24**, 101223 (2019).
31. Lizarbe, B. *et al.* High-fat diet consumption alters energy metabolism in the mouse hypothalamus. *Int J Obes*, **43**, 1295–1304 (2019).
32. Albrecht, J., Sidoryk-Węgrzynowicz, M., Zielińska, M. & Aschner, M. Roles of glutamine in neurotransmission. *Neuron Glia Biol*, **6**, 263–276 (2010).
33. Wilson, M., Reynolds, G., Kauppinen, R. A., Arvanitis, T. N. & Peet, A. C. A constrained least-squares approach to the automated quantitation of in vivo ^{1}H magnetic resonance spectroscopy data. *Magn Reson Med*, **65**, 1–12 (2011).
34. Siddiqui, M. S. *et al.* Case definitions for inclusion and analysis of endpoints in clinical trials for nonalcoholic steatohepatitis through the lens of regulatory science., **67**, 2001–2012 (2018).
35. Bedossa, P. *et al.* Histopathological algorithm and scoring system for evaluation of liver lesions in morbidly obese patients., **56**, 1751–1759 (2012).
36. Musolino, V. *et al.* The synergistic effect of Citrus bergamia and Cynara cardunculus extracts on vascular inflammation and oxidative stress in non-alcoholic fatty liver disease. *J Tradit Complement Med*, **10**, 268–274 (2020).
37. Younossi, Z. M. *et al.* Global epidemiology of nonalcoholic fatty liver disease-Meta-analytic assessment of prevalence, incidence, and outcomes.*Hepatology* **64**,73–84(2016).
38. Younossi, Z. M. *et al.* The global epidemiology of NAFLD and NASH in patients with type 2 diabetes: A systematic review and meta-analysis. *J Hepatol*, **71**, 793–801 (2019).
39. Castro, R. E. & Diehl, A. M. Towards a definite mouse model of NAFLD. *J Hepatol*, **69**, 272–274 (2018).
40. Gliozzi, M. *et al.* Cholesterol homeostasis: Researching a dialogue between the brain and peripheral tissues. *Pharmacol Res*, **163**, 105215 (2021).
41. Scarano, F. *et al.* Potential of Nutraceutical Supplementation in the Modulation of White and Brown Fat Tissues in Obesity-Associated Disorders: Role of Inflammatory Signalling. *Int J Mol Sci*, **22**, 3351

(2021).

42. Mondal, A. *et al.* Lipocalin 2 induces neuroinflammation and blood-brain barrier dysfunction through liver-brain axis in murine model of nonalcoholic steatohepatitis. *J Neuroinflammation*, **17**, 201 (2020).
43. Lyn-Cook, L. E. *et al.* Hepatic ceramide may mediate brain insulin resistance and neurodegeneration in type 2 diabetes and non-alcoholic steatohepatitis. *J Alzheimers Dis*, **16**, 715–729 (2009).
44. de la Monte, S. M., Longato, L., Tong, M. & Wands, J. R. Insulin resistance and neurodegeneration: roles of obesity, type 2 diabetes mellitus and non-alcoholic steatohepatitis. *Curr Opin Investig Drugs*, **10**, 1049–1060 (2009).
45. Oshida, K. *et al.* Effects of dietary sphingomyelin on central nervous system myelination in developing rats. *Pediatr Res*, **53**, 589–593 (2003).
46. Li, Y. H., Woo, S. H., Choi, D. H. & Cho, E. H. Succinate causes α-SMA production through GPR91 activation in hepatic stellate cells. *Biochem Biophys Res Commun*, **463**, 853–858 (2015).
47. Krols, M., Bultynck, G. & Janssens, S. ER-Mitochondria contact sites: A new regulator of cellular calcium flux comes into play. *J Cell Biol*, **214**, 367–370 (2016).
48. Lauwers, E., Goodchild, R. & Verstreken, P. *Membrane Lipids in Presynaptic Function and Disease. Neuron*, **90**, 11–25 (2016).
49. van Echten-Deckert, G. & Alam, S. Sphingolipid metabolism - an ambiguous regulator of autophagy in the brain. *Biol Chem*, **399**, 837–850 (2018).
50. Duarte, N. *et al.* How Inflammation Impinges on NAFLD: A Role for Kupffer Cells. *Biomed Res Int* 2015, 984578 (2015).
51. Moffett, J. R., Arun, P., Ariyannur, P. S. & Namboodiri, A. M. N-Acetylaspartate reductions in brain injury: impact on post-injury neuroenergetics, lipid synthesis, and protein acetylation. *Front Neuroenergetics*, **5**, 11 (2013).
52. Bowser, T. E. & Trawick, M. L. Probing the specificity of gamma-glutamylamine cyclotransferase: an enzyme involved in the metabolism of transglutaminase-catalyzed protein crosslinks., **44**, 143–150 (2013).
53. Norenberg, M. D. Distribution of glutamine synthetase in the rat central nervous system. *J Histochem Cytochem*, **27**, 756–762 (1979).
54. Bernstein, H. G. *et al.* Reduced density of glutamine synthetase immunoreactive astrocytes in different cortical areas in major depression but not in bipolar I disorder. *Front Cell Neurosci*, **9**, 273 (2015).
55. Limón, I. D., Angulo-Cruz, I., Sánchez-Abdon, L. & Patricio-Martínez, A. Disturbance of the Glutamate-Glutamine Cycle, Secondary to Hepatic Damage, Compromises Memory Function. *Front Neurosci*, **15**, 578922 (2021).
56. Schönfeld, P. & Reiser, G. Why does brain metabolism not favor burning of fatty acids to provide energy? Reflections on disadvantages of the use of free fatty acids as fuel for brain. *J Cereb Blood*

Flow Metab, **33**, 1493–1499 (2013).

57. McPherson, P. A. & McEneny, J. The biochemistry of ketogenesis and its role in weight management, neurological disease and oxidative stress. *J Physiol Biochem*, **68**, 141–151 (2012).
58. Puchalska, P. & Crawford, P. A. Multi-dimensional Roles of Ketone Bodies in Fuel Metabolism, Signaling, and Therapeutics. *Cell Metab*, **25**, 262–284 (2017).
59. Romano, A. *et al.* Fats for thoughts: An update on brain fatty acid metabolism. *Int J Biochem Cell Biol*, **84**, 40–45 (2017).
60. Panov, A., Orynbayeva, Z., Vavilin, V. & Lyakhovich, V. Fatty acids in energy metabolism of the central nervous system. Biomed Res Int 2014, 472459 (2014).

Figures

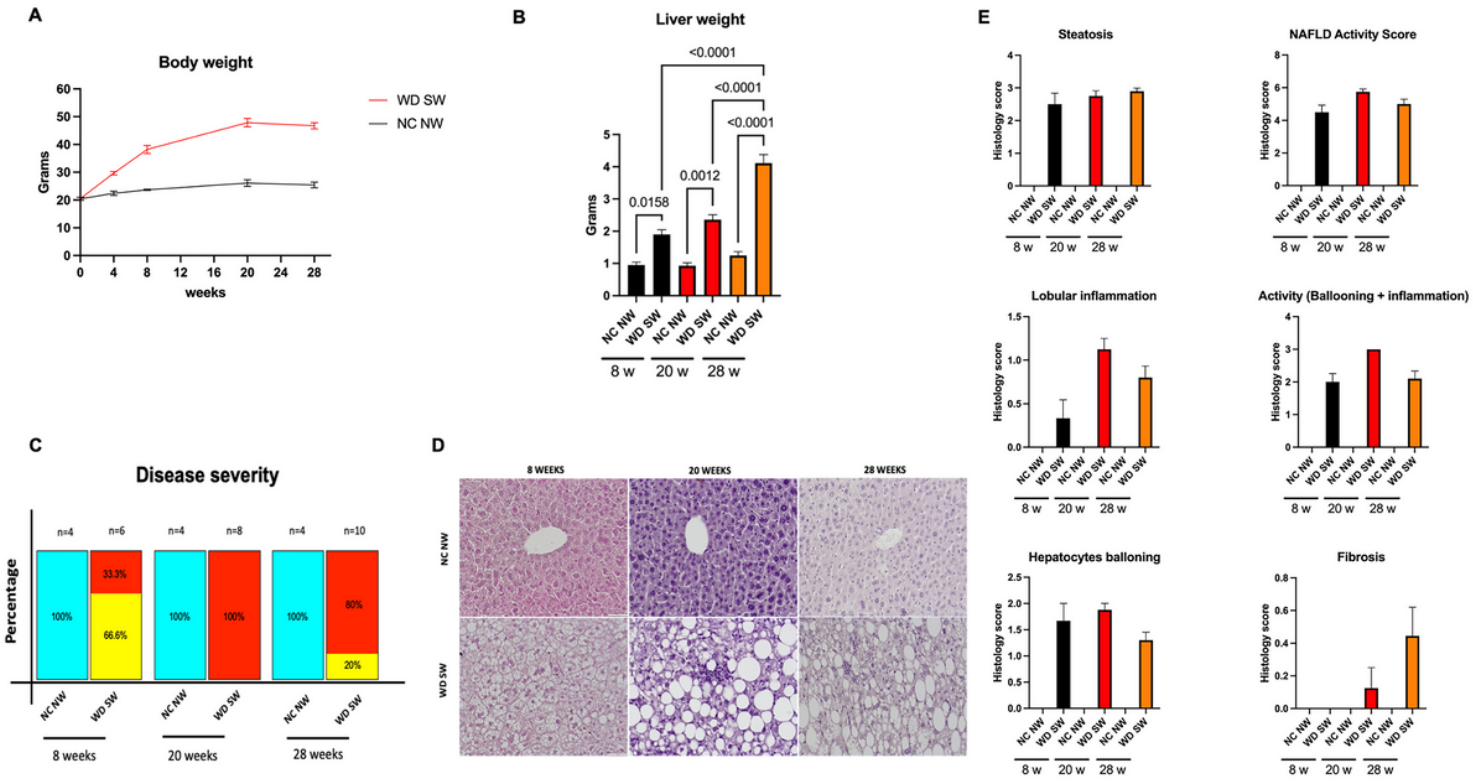

Figure 1

High-fat diet-fed mice develop fatty liver and steatohepatitis. (A) body change over time. Animals were fed a normal chow diet and tap water (NC NW) or high fructose/glucose, high fat Western Diet (WD SW) for up to 28 weeks. (B) High fat Western Diet was associated with a significant increase in terminal liver weight compared to CD NW-fed animals at 8, 20 and 28 weeks. (C) Disease severity expressed in percentage. (D) Gross liver from DIAMOND mice fed a control diet (NC NW) or high high fat Western Diet (WD SW) for 8, 20 and 28 weeks. Representative liver sections stained with hematoxylin-eosin (H&E) of livers from CD NW or WD SW mice at 8, 20 or 28 weeks of diet are shown. Original magnification, ×20. (E) Histology score for steatosis, hepatocyte ballooning, lobular inflammation, fibrosis and NAFLD Activity

Score were quantified. Data are expressed as the mean ± SEM for 4–10 mice per group. For body weight NC NW AUC=683.1±20.2; WD SW AUC=1131±50.2. WD SW AUC<0.001 vs NC NW AUC.

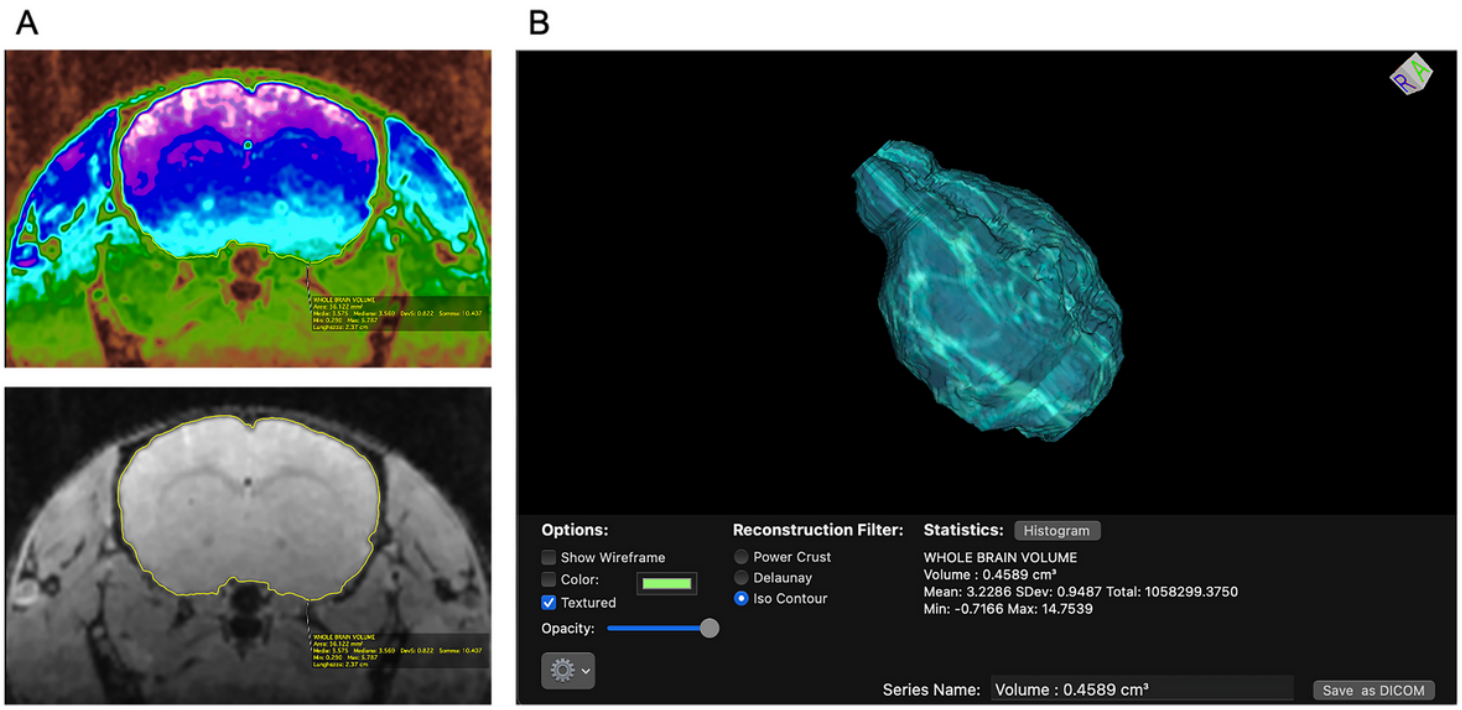

Figure 2

Volumetric analysis. (A) Region of interest-to-volume feature on OsiriX Imaging Software. (B) Compute ROI Volume feature of OsiriX used to compute the volume.

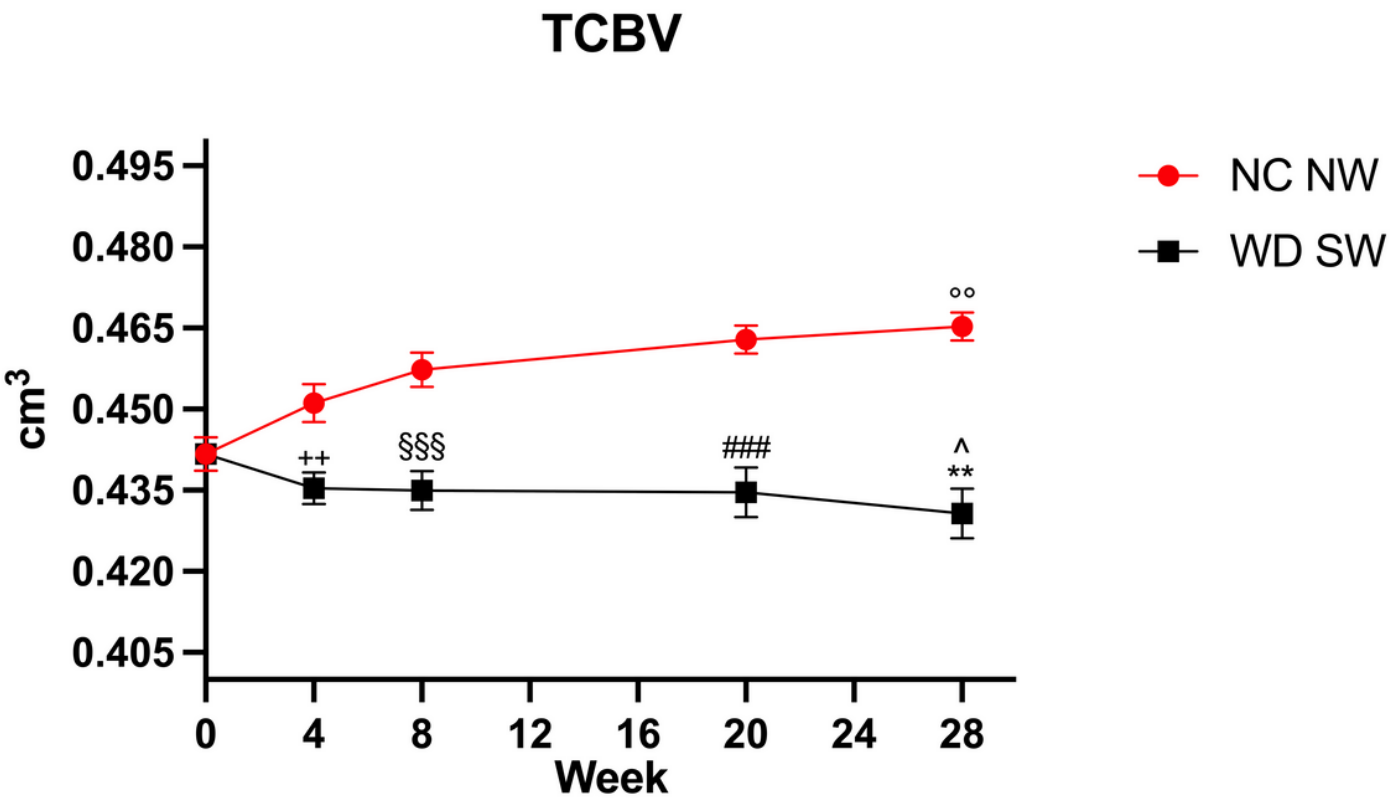

Figure 3

Total cerebral brain volume for the NC NW (red) and WD SW (black) mice during the 24 weeks investigated. T0: 0 weeks, T1: 4 weeks, T2: 8 weeks, T3: 20 weeks, T4: 28 weeks. The results are expressed as mean ± S.E.M. ^: p<0.05 vs WD SW T0, **: p<0.01 vs NC NW T4, °°: p<0.01 vs NC NW T0, ++: p<0.01 vs NC NW T1, §§§: p<0.001 vs NC NW T2, ###: p<0.001 vs NC NW T3. NC NW: Normal Chow Normal Water, WD SW: Western Diet Sugar Water.

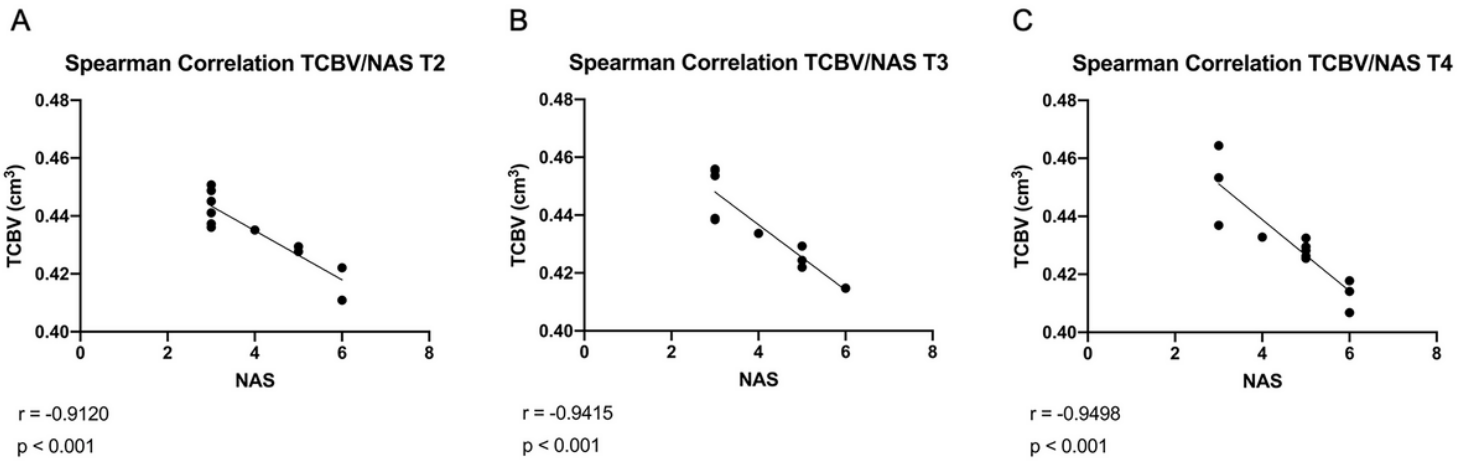

Figure 4

Relationship between TCBV (Total cerebral brain volume, cm3) and NAS (NAFLD Activity Score, 0-8) by Spearman-related analysis. Lines are generated using regression analysis (GraphPad Prism); r = Spearman's correlation coefficient; NAS represents the sum of scores for steatosis, lobular inflammation and ballooning; T2: 8 weeks; T3: 20 weeks; T4: 28 weeks.

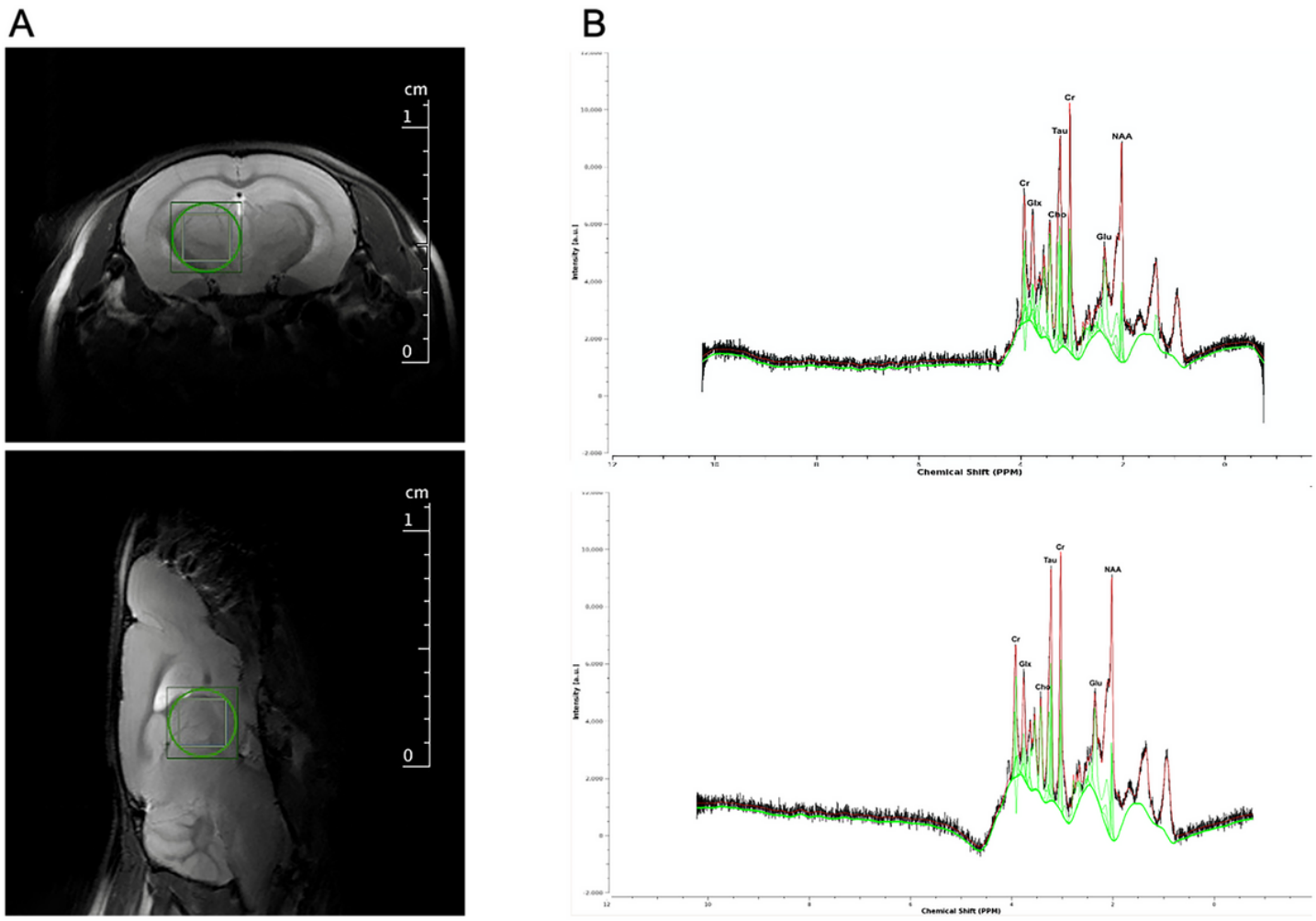

Figure 5

1H-MRS of the mouse thalamus. (A) Representative axial and sagittal T2_turboRARE weighted images with fat suppression of mouse brain and corresponding voxel location centered in the thalamic region (2x2x2 mm3). (B) Representative in vivo 1H-MRS spectra from NC NW mouse thalamus (top) and WD SW mouse thalamus (bottom) performed by Tarquin.

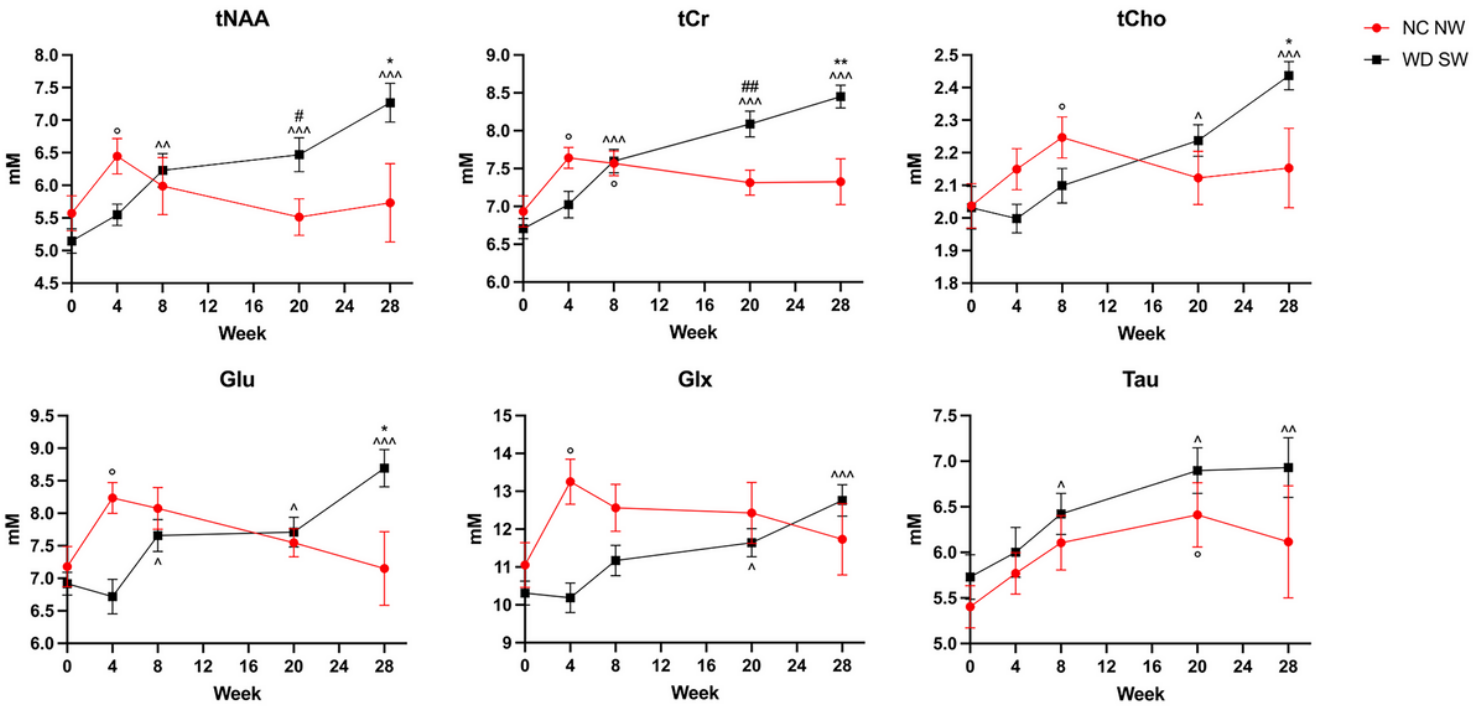

Figure 6

Concentration values of the metabolites for NC NW (red) and WD SW (black) mice during the 24 weeks investigated. The results are expressed as mean ± S.E.M. *: p<0.05, **: p<0.01 vs NC NW T4; #: p<0.05, ##: p<0.01 vs NC NW T3; ^: p<0.05, ^^: p<0.01, ^^^: p<0.001 vs WD SW T0; °: p<0.05 vs NC NW T0. NC NW: Normal Chow Normal Water, WD SW: Western Diet Sugar Water; T0: 0 weeks, T1: 4 weeks, T2: 8 weeks, T3: 20 weeks, T4: 28 weeks. tNAA, total N-acetylaspartate; tCr, total creatine; tCho, total choline; Glu, glutamate; Glx, glutamate + glutamine; Tau, Taurine.